A Tapered Phased Array Ultrasound Transducer for Hyperthermia Treatment

PAUL J. BENKESER, MEMBER, IEEE, LEON A. FRIZZELL, SENIOR MEMBER, IEEE, KENNETH B. OCHELTREE, MEMBER, IEEE, AND CHARLES A. CAIN, SENIOR MEMBER, IEEE

Abstract—**An ultrasonic tapered phased array transducer, consisting of a linear phased array employing elements with a tapered thickness, was developed to study the feasibility of its use for hyperthermic treatment of deep-seated tumors. The cylindrical focal region is generated and steered in two dimensions by controlling the phases of the driving signals on each element and moved in the third dimension by changing the driving frequency. Experimentally obtained field intensity distributions are in good agreement with theoretical predictions. Acoustical power output measurements indicate that tapered phased arrays are capable of providing the intensities necessary for producing therapeutic temperatures in tumors.**

I. Introduction

THE USE of hyperthermia in the treatment of cancer had its origin in the medical practices of Roman physicians, such as Hippocrates, as early as 2000 BC [1]. Interest in hyperthermia was renewed in the late 1800's due to research by W. Busch in 1866 on heat-related tumor regressions [1] but diminished with the discovery of X rays and the use of radiotherapy in the treatment of cancer. Within the past decade, however, there has been a renewed interest in hyperthermia based on research indicating that cancer cells are more sensitive to increased temperatures (42–45°C) than are normal cells. Most data available to date indicate that reduced tumor *p*H, position in the cell growth cycle, and decreased nutrient supply are among the more important factors in determining the intrinsic sensitivity of tumor cells to hyperthermia [1]. Fortunately, cells that are heat resistant are often the most sensitive to radiation therapy [2]. In fact, the synergistic effect of hyperthermia and radiation therapy has been well documented and is perhaps the most useful application of hyperthermia [3], [4].

Many different modalities, such as microwaves, ultrasound, and radio frequency currents, have been used to produce local hyperthermia. Each of these techniques has different physical constraints that can limit its applicability to particular tumor locations. The intensity of unfocused high-frequency microwaves (400–2450 MHz) is reduced by a factor of e^{-1} at depths of only 1–3 cm, due to high absorption in the tissue [5]. Focusing the microwave energy at these frequencies can increase the depths of penetration to 5 or 6 cm. Lower frequency microwaves (10–50 MHz) can penetrate to depths of approximately 12 cm but because of the long wavelengths (37 to 185 cm) cannot be focused for localization within the body [5].

Ultrasound, in the 0.3- to 3.0-MHz frequency range, has several properties that favor its use in localized hyperthermia. Due to its short wavelength and favorable absorption characteristics, ultrasonic energy can be focused into a smaller region and achieve a greater depth of penetration than can microwave energy [6]. As a result of this focusing advantage, ultrasound is capable of creating a temperature rise in a tumor deep inside the body which is more uniform and controllable than that produced by microwave energy [7].

The disadvantages of using ultrasound for hyperthermia are primarily related to impedance mismatches that are present at tissue–air or tissue–bone interfaces and the high absorption of ultrasound in bone (approximately 15 times greater than that of soft tissues [8]). Ultrasound is almost totally reflected at tissue–air interfaces, which can result in standing waves or scattering and increased attenuation of the ultrasound, depending upon the size and shape of the air pockets. Local hot spots at tissue–bone interfaces can result from both the high longitudinal attenuation and mode conversion from longitudinal to even more highly attenuated shear waves [8]. This is a common clinical problem that can result in an aborted treatment if the patient experiences excessive pain [9].

There are several ultrasound systems currently being used to produce deep localized hyperthermia, some of which employ multiple transducers arranged so that their fields overlap within the tumor volume. A recently developed system uses 30 focused transducers mounted in a hexagonal configuration [10]. The individual transducers, as well as the entire array of transducers, can be positioned mechanically to control the shape and position of the system focal region. Clinical data from the use of this system are limited since it has only recently been developed, and critical evaluations of its performance are not yet available.

Another multiple transducer system, employing six unfocused transducers, has been used in clinical trials [11].

Manuscript received April 21, 1986; revised August 14, 1986. This work was supported in part by Labthermics Technologies, Inc., and NIH Training Grant CA 09067.

P. J. Benkeser is with the School of Electrical Engineering, Georgia Institute of Technology, Atlanta, GA 30332-0250.

L. A. Frizzell, K. B. Ocheltree, and C. A. Cain are with the Bioacoustics Research Laboratory, University of Illinois, 1406 W. Green Street, Urbana, IL 61801.

IEEE Log Number 8612855.

The configuration of the transducers can be manipulated prior to the treatment to adjust the system focal region, but the unit must remain fixed in space for the duration of the treatment. The major problem with this system has been the inability to control or modify, during treatment, the deposition of the ultrasonic energy used for heating. This usually results in the development of hot spots in the normal tissues surrounding the tumor which can produce pain intolerable to the patient and cause the treatment to be terminated prematurely [12]. Due to the large size of the transducer assembly, both of these multiple transducer systems require large acoustic access windows to treat tumors at appreciable depths.

A mechanically scanned focused transducer has also been used to produce deep localized ultrasound hyperthermia [7], [13]. The focal region is swept in a predetermined scan path, usually around the periphery of the tumor, by moving the transducer. To achieve preferential heating at the tumor with this system, the radiating area of the transducer must be large compared to the cross section of its focal region [14].

None of the systems currently used for treating deep-seated tumors is capable of three-dimensional focal region placement without some type of mechanical movement of the transducers. Clearly, new types of ultrasonic transducers that can more accurately and efficiently heat deep-seated tumors while minimizing the heating of surrounding normal tissues are needed. An alternative approach to mechanical alignment of multiple transducers or mechanical scanning of one or more transducers is to use an ultrasonic phased array. A phased array offers the alternative of electronic scanning of a focused beam without movement of the transducer assembly. The focus can be generated and positioned in three dimensions by controlling the phases of the signals driving each array element so that constructive interference is achieved at the desired field point. By readjusting the phases periodically, the focus can be scanned over any three-dimensional path at a rate much faster than that of a mechanically scanned system. The short time between scans can result in a smaller temperature variation at any location. Also, the scan path can be changed quickly to maintain the desired normal and tumor tissue temperatures.

The complexities of phase control, many amplifiers, and complex fabrication techniques can be reduced if, instead of a complete two-dimensional array of elements, a stacked linear phased array [15], or a one-dimensional phased array composed of elements that have a tapered thickness [16], [17] is employed. Herein we are concerned with the latter type which is illustrated in Fig. 1. The region along the length of the element that has a thickness resonant at the frequency of the driving signal will produce the greatest acoustical power output. Thus different regions along the length of the element can be excited by changing the frequency of the continuous wave (cw) signal driving the element. Frequency shifting has been used in other transducer designs to produce beam movement [18]. A tapered phased array allows the focal region to be swept in two dimensions by controlling the phases of the cw signals and in the third dimension by controlling the frequency of those signals. This tapered array would have the square root of N elements compared with N elements for a two-dimensional array with the same center-to-center spacing of elements. This paper discusses the design considerations and the results from initial testing of a tapered phased array transducer to determine the feasibility of using such a transducer for hyperthermia treatment.

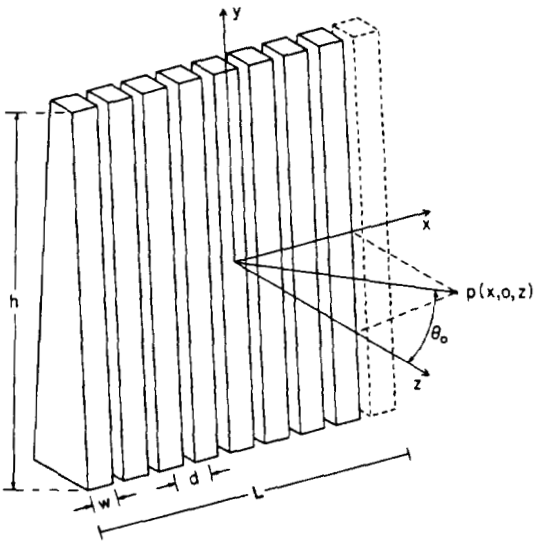

Fig. 1. Diagram of ultrasonic tapered phased array.

II. Theory

The dimensions associated with the tapered phased array elements are shown in Fig. 1. The height of an element h corresponds to its dimension in the y direction. The element width and center-to-center spacing are w and d, respectively. The overall length of the array in the x direction is L. The steering angle θ_0 is the angular position of the focus with respect to the $x = 0$ plane.

The element center-to-center spacing d is of particular interest since it affects the location of the grating lobes which, in general, can appear in the real or visible region ($-90° < \theta < 90°$, where θ is the observation angle) in addition to the main lobe and its side lobes. The grating lobes also result from constructive interference from each element, and their presence, for a fixed acoustical power output, decreases the energy in the focal region [19]. The angular location of the nth grating lobe ϕ_n is given by

$$\phi_n = \sin^{-1}\left(\frac{\lambda n}{d}\right) \tag{1}$$

where ϕ_n is in the $y = 0$ plane, λ is the wavelength, and $n = \pm 1, \pm 2, \pm 3$, etc., specifies the order of the grating lobe. When a beam steering angle of θ_0 is introduced, the angular location of the nth grating lobe is given by

$$\phi_n = \sin^{-1}\left(\frac{\lambda n}{d} - \sin\theta_0\right). \tag{2}$$

From this relation the position for the nth-order grating lobe along x for constant $z = z_0$ is approximately

$$x_n = z_0 \tan\left(\sin^{-1}\left(\frac{\lambda n}{d} - \sin\theta_0\right)\right). \tag{3}$$

If d is equal to λ, the grating lobes will be absent for a steering angle of 0°, but they will be present for a nonzero value of θ_0 and will increase in amplitude with increasing magnitude of θ_0 [19]. On the other hand, if $d < \lambda/2$, then no grating lobes will exist for any steering angle. Since grating lobes are a result of the periodic spacing of the array elements, they may also be avoided by spacing the elements unequally. However, the sidelobe amplitudes in these aperiodic arrays are significantly increased [20].

To minimize the number of elements and associated phasing and amplifier hardware for an array of fixed length L and to maximize the acoustical power output from an element, it is desirable to make the elements as wide as possible without significantly decreasing the energy in the focal region. To accomplish this, the ratio of wavelength to center-to-center spacing λ/d should be made greater than the value of $\sin\theta_0$ for the maximum beam steering angle. For example, if the largest tumor to be treated is 5 cm in diameter and is located at a minimum depth of 10 cm, the largest steering angle required is approximately 14°. From (2) with $d = 0.8\lambda$, the focus can be steered off axis by 14° without the center of the first grating lobe appearing in the visible field. Therefore, using a center-to-center spacing of 0.8λ instead of $\lambda/2$ would decrease the total number of elements in the array without decreasing the energy in the focused main lobe.

The region of excitation for the tapered array will be centered on that portion of the element having a thickness resonant at the applied frequency. The extent of the region of excitation in the y direction is determined by the rate of taper and by the mechanical quality factor Q_m of the ceramic. A crude approximation of Q_m for an air-backed transducer is given by

$$Q_m = \frac{\pi\rho_m c_m}{2\rho_0 c_0} \tag{4}$$

where $\rho_m c_m$ is the product of density and sound velocity in the transducer material, and $\rho_0 c_0$ is the product of density and sound velocity in the loading medium [21]. However, losses within the material, mounting losses, and the narrow width of the elements cause the actual Q_m to be significantly lower than the value computed using (4). These additional losses reduce the energy radiated by the elements.

The theoretical determination of the intensity field patterns of the array must include the variations in the output along the height of the tapered elements. First, consider the electrical analog of a lossless mechanical piezoelectric transducer of uniform thickness near resonance as shown in Fig. 2(a) [22]. The acoustic power radiated by the transducer is analogous to the average power dissipated

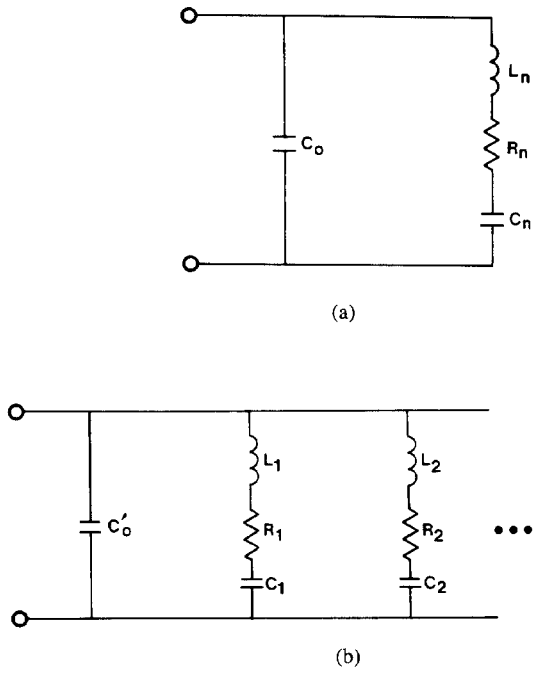

Fig. 2. Equivalent electrical circuits of piezoelectric transducers. (a) Uniform thickness. (b) Tapered thickness.

in R_n. In terms of the properties of the ceramic and radiation medium, R_n can be expressed as

$$R_n = \frac{\rho_0 c_0 d_n^2}{2e_{11} S} \tag{5}$$

where ρ_0 and c_0 are, respectively, the density and speed of sound in the radiation (loading) medium, d_n is the ceramic thickness, e_{11} is the piezoelectric constant, and S is the equivalent radiating surface area of the ceramic [22]. At resonance the equivalent electrical circuit of the transducer will look like a resistance R_n in parallel with a capacitance C_0. The tapered element can be modeled using a distributed network of these equivalent circuits, as shown in Fig. 2(b). The capacitance C_0' is the equivalent parallel capacitance of all of the branches of the network. The impedance of one resistance-inductance-capacitance (RLC) branch of this model can be expressed as

$$Z_n(j\omega) = R_n\left[1 + jQ_m\left(\frac{\omega}{\omega_n} - \frac{\omega_n}{\omega}\right)\right] \tag{6}$$

where

$$\omega_n = \frac{1}{(L_n C_n)^{1/2}}$$

is the resonance frequency of the nth branch. When the network is driven by a signal of frequency $\omega = \omega_1$, the position along the height of the element corresponding to the branch with $\omega_n = \omega_1$ will generate the greatest acoustical power output. The relative radiated power W_n from R_n in any branch can be expressed as

$$W_n = V^2\left[\frac{R_n^2}{|Z_n|^2}\right] \tag{7}$$

where V is the voltage applied to the element. Except for the thickness d_n of the ceramic, the remaining parameters in (5) will be independent of the y position along the element. Equation (5) can be rewritten in terms of the corresponding resonance frequency ω_n of the branch containing R_n as

$$R_n = \frac{\rho_0 c_0}{2e_{11}S}\left(\frac{\pi^2 c^2}{\omega_n^2}\right) \tag{8}$$

where c is the speed of sound in the ceramic. Substituting (8) and (6) into (7) yields

$$W_n = K\left[\frac{\omega_n^2}{\left|1 + jQ_m\left(\frac{\omega}{\omega_n} - \frac{\omega_n}{\omega}\right)\right|^2}\right] \tag{9}$$

where

$$K = \frac{2V^2 e_{11} S}{\pi^2 \rho_0 c_0 c^2}.$$

From (6) it is clear that the impedance for all of the branches, except for the resonant branch, will be complex. This will result in a phase shift of the current with respect to the applied voltage. Thus the phase of the acoustic pressure will vary along the y direction of the element. This phase shift ψ derived from (6) can be expressed as

$$\psi = \tan^{-1}\left(Q_m\left(\frac{\omega}{\omega_n} - \frac{\omega_n}{\omega}\right)\right). \tag{10}$$

Using (9) and (10), the relative magnitude and phase of the acoustic output along the height of an element can be calculated.

III. Design and Fabrication

An important design consideration for the tapered phased array, and indeed any hyperthermia applicator, is the intensity gain required to preferentially heat the tumor. Without preferential heating, normal as well as tumor tissues will be heated to therapeutic temperatures. The array must provide time-averaged intensity gain so that the intensity, averaged over a complete scan of the tumor, is greater at the tumor location than at the body surface and all other locations within intervening normal tissues. This gain, G_{ta}, is defined as the ratio of the time-averaged intensity at the tumor center to the time-averaged intensity at the body surface. Assuming for this analysis that the time-averaged intensities at the body surface and at the tumor are uniform in the x direction, a G_{ta} greater than one is obtained by making the length of the array long compared to the tumor diameter [15].

The results of several theoretical studies of tumor heating using scanned focused ultrasound at 500 kHz have been reported. One study indicated that a 2.4-cm-diameter tumor located 4.3 cm in depth could be heated to 43°C with minimal heating in normal tissues by a focused beam with a time-averaged intensity gain of approximately 2.4 dB [14]. Another study showed that a 4-cm-diameter tumor at a depth of 13 cm could be heated to 43°C with a time-averaged intensity gain of 4.8 dB [23]. Based on these theoretical intensity gains, a G_{ta} of 3.0 dB was chosen for the tapered phased array.

To calculate the array length necessary to heat selectively a tumor of a given size, one must consider the following: 1) losses due to attenuation incurred along the path from the transducer to the tumor; 2) increased path length from elements at the ends of the array; 3) directionality of the elements; and 4) phase quantization errors. Phase quantization errors are introduced into the system when digital signal-processing systems are used to produce the phase shifts necessary for focusing and steering. All of these factors are best considered by calculating the intensity field distribution produced by an array. A computer program was developed previously for this purpose [24]. The program divides the elements of the array into subelements that are small enough so that their fields can be represented, in the region of interest, by the far-field approximation. The effect of the tapered elements was taken into account by weighting the magnitude and phase of the acoustic output of each subelement along the height of the element using the results from (9) and (10), respectively. The total acoustic pressure at a specific point in the field was determined by summing the contributions at that point from each of the subelements after correcting for attenuation.

Using this model the maximum treatable tumor diameter can be determined when the frequency, array length, and desired G_{ta} are specified. The gain in intensity at the focus relative to that near the surface of the array G_f including the effect of attenuation, can be determined from a plot of intensity versus distance from the array. This gain is large since such a plot does not consider the time-averaging resulting from scanning the beam in the x direction. This time-averaging effect is considered by multiplying G_f (expressed as a ratio) by the 3-dB beamwidth in the x-direction. However, G_f must first be adjusted for the desired G_{ta}, defined previously, to yield the corrected gain G_c given by

$$G_c = G_f - G_{ta}. \tag{11}$$

Thus the maximum treatable tumor diameter D is approximately given by

$$D = B \times 10^{(0.1G_c)} \tag{12}$$

where B is the 3-dB beamwidth in the x direction and all gains are expressed in decibels [15].

For a tapered phased array with an array length of 12.63 cm and an element center-to-center spacing of 1.97 mm, operating at a frequency of 650 kHz (attenuation coefficient, A = 0.1 Np/cm/MHz), the field intensity for points close to the array is approximately 14 dB below the intensity at the focus resulting in a G_f of 14 dB. A corrected gain G_c of 11.0 dB is calculated from (11), based on a G_{ta} of 3-dB. The 3-dB beamwidth of the focus at 650 kHz is approximately 0.17 cm. Therefore, the maximum

treatable tumor diameter is 2.1 cm at a depth of 8 cm, as calculated from (12).

To obtain the intensity gain necessary to treat tumors larger than 2.1 cm, the array would have to operate at lower frequencies at which the losses due to attenuation in the intervening normal tissue are less, thereby increasing the intensity gain G_f. However, the choice of the operating frequency range cannot be too low because significant heating behind the tumor could occur. Many factors such as the normal and tumor absorption coefficients, perfusion levels in the tumor and surrounding tissue, and presence of bone behind the tumor will determine the minimum frequency that may be used. Based on the simulations of scanned focused ultrasound, it appears that frequencies in the neighborhood of 500 kHz could be used without excessive heating of the surrounding normal tissues [14], [23]. For a tapered array operating at 500 kHz, with the same element spacings and array length as before, the maximum treatable tumor diameter is 4.0 cm, nearly double that at 650 kHz.

The fabrication techniques employed for hyperthermia phased arrays are somewhat different from those for producing linear phased arrays for imaging since the former operate with cw signals so that the damping provided by a backing material is not only unnecessary, but undesirable because of the resulting reduction of efficiency. A tapered phased array was fabricated from a 15.2 × 15.2 cm lead zirconate titanate ceramic plate with a tapered thickness of 4.3–5.8 mm, corresponding to a frequency range of 650–850 kHz. The plate was cut into 64 strips, 1.79 mm ($\pm$10 percent) wide. The variations in width resulted from errors in positioning the saw blade used to cut the ceramic. The 64 elements were mounted, air-backed, in an anodized aluminum housing, with a center-to-center spacing of 1.97 mm. Since only 32 RF power amplifiers were available for this study, all measurements were made using only 32 elements of the array.

When a tapered ceramic plate is cut into narrow elements, the resonance frequency range will no longer be determined by the common thickness mode resonance, as is the case when the width of the ceramic is substantially larger than its thickness. Instead, the thickness dilatational mode, which occurs when the width of the ceramic is less than its thickness, will be the dominant resonance mode. The measured resonant frequency range of the array was approximately 500–700 kHz. For this range of frequencies the element center-to-center spacing, in terms of wavelength, varied from 0.60 to 0.85 λ.

IV. Experimental Techniques

The acoustical power output of the tapered phased array transducer was determined by measuring the radiation force exerted on a reflecting target. The target was 7.6 × 5.1 × 0.3 cm and consisted of approximately 200-μm-thick brass plates bonded to each side of an open rectangular Plexiglas frame, forming an air gap between the plates which made the target virtually a perfect reflector. The target was suspended at an angle of 45° to the incident field by small diameter nylon threads and enclosed by a Plexiglas frame with acoustic windows (5-μm-thick polyethylene) in the front and rear to prevent convection and acoustic streaming from affecting the response of the target.

The total acoustic power incident on the target W was determined from

$$W = \frac{mgcd}{(L^2 - d^2)^{1/2}} \tag{13}$$

where m is the mass of the target, corrected for buoyancy, g is the acceleration of gravity, L is the length of the suspension, c is the speed of sound, and d is the horizontal deflection of the target which occurs when the sound is present. The deflection d was measured with a cathotometer to an accuracy of 0.2 mm.

To determine the electrical power delivered to the array, the input electrical power from the amplifier's dc power supply was measured. The total electrical power delivered to the array, based on the average efficiency of the amplifiers, was approximately 80 percent of the input power from the supply.

Field intensity profiles were determined by mounting the transducer inside a 50-l Plexiglas tank filled with degassed water and lined with sound absorbing material. The tank was mounted on a milling base where movement in three rectangular coordinate directions could be either controlled manually or by a computer. A hydrophone probe, consisting of a 1-mm-diameter 20-MHz PZT-5A ceramic disk mounted at the tip of a rigid coaxial rod, was used to observe the acoustic field pressure produced by the transducer. The output of the hydrophone probe was amplified and measured using a digital voltmeter with an analog dc output. The analog output signal was routed to a 25-kHz analog-to-digital converter connected to a Perkin Elmer 7/32 minicomputer. The minicomputer was programmed to move the tank and transducer continuously in the desired coordinate direction and to record the voltage from the hydrophone at 2-mm intervals. These data were squared and converted to decibels relative to the peak amplitude for storage on magnetic tape as relative intensity.

V. Results

Fig. 3 shows a comparison of the experimental and theoretical field profiles in the x direction at z = 100 mm for the tapered phased array developed for this study operating at 650 kHz. The focus is steered off axis by 2.5 cm. Fig. 4 shows the experimental and theoretical profiles in the z direction with the focus on axis (x = 0). These two figures illustrate the good agreement between the theoretically predicted fields and the experimental data for the focal region. The differences in the sidelobe intensities are attributable to the variations in output of the individual elements due to their impedance differences. There was typically a 15-percent variation in the magnitudes and a $\pm$5° variation in the phases of the element imped-

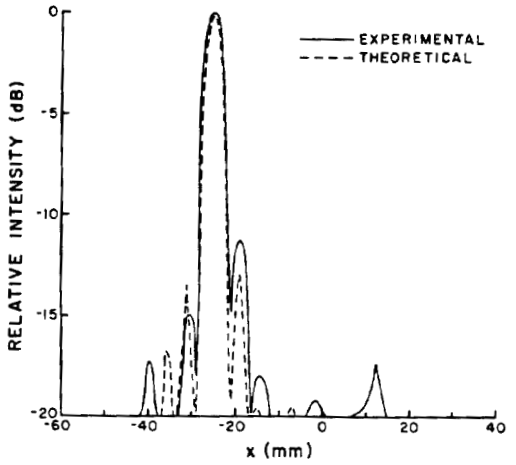

Fig. 3. Comparison of theoretical and experimental field profiles in x direction at $y = 50$ mm ($f = 650$ kHz) and $z = 100$ mm. Focus at (−25, 50, 100) mm.

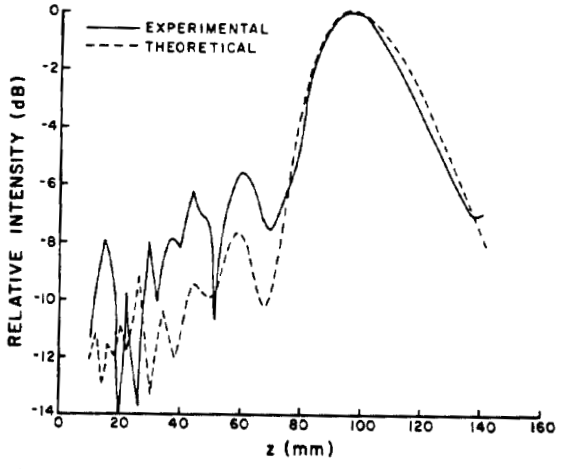

Fig. 4. Comparison of theoretical and experimental field profiles in z direction at $y = 50$ mm ($f = 650$ kHz) and $x = 0$. Focus at (0, 50, 100) mm.

ances. Since the impedance of an element is proportional to its width [22], the measured ten-percent variation in width of the elements would seem to account for most of the impedance differences. Nonuniformity of the properties of the ceramic material such as density, speed of sound, and polarization would also contribute to the impedance variations. The variation in the magnitudes of the impedances would result in an approximately 15-percent change in the acoustical power outputs of the elements assuming each were driven by the same voltage. In linear arrays manufactured for imaging, such variations in sensitivity (power output) and delay errors (phase errors) cause the side lobes to increase in number and amplitude, and to be asymmetrical [25]. The main lobe, however, is not significantly affected.

Fig. 5 shows a comparison of the intensity profiles in the y direction at 580, 620, and 650 kHz. In comparing the three profiles, it is clear that a frequency shift from 580 to 650 kHz moves the beam approximately 6 cm in the y direction. The theoretical predictions were based on a Q_m of 8 for the 580 and 620 kHz cases, and a Q_m of 11

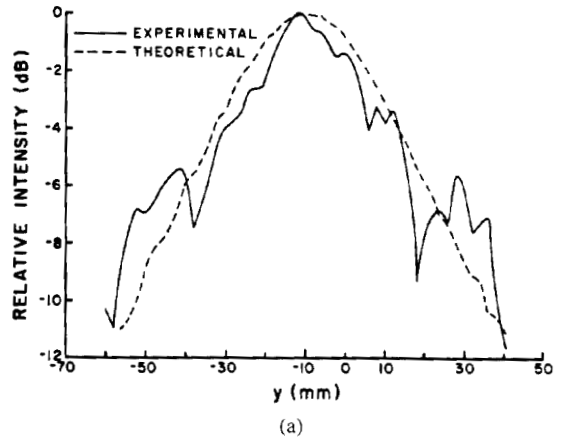

(a)

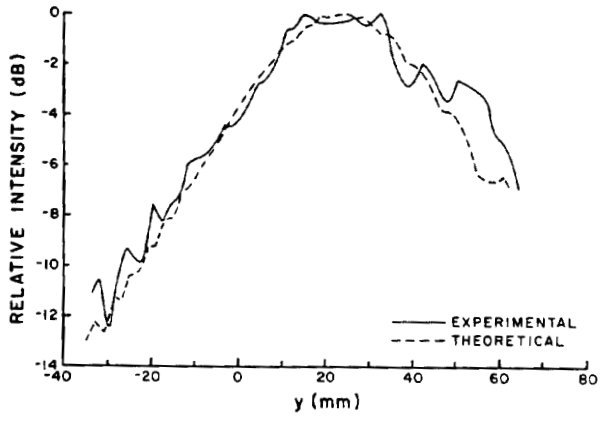

(b)

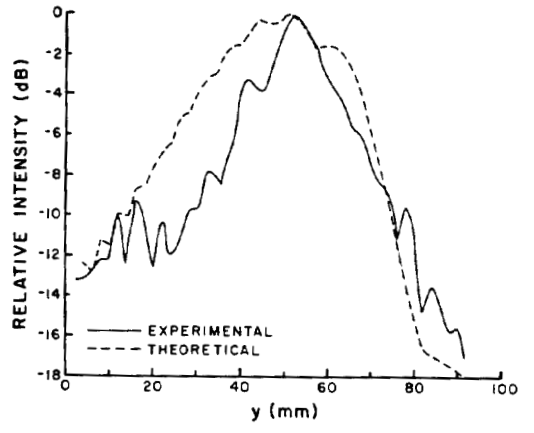

(c)

Fig. 5. Comparison of theoretical and experimental field profiles in y direction ($x = 0$, $z = 100$ mm). (a) $f = 580$ kHz. (b) $f = 620$ kHz. (c) $f = 650$ kHz.

for the 650 kHz case. The Q_m at 650 kHz was greater to simulate the damping from the clamped end of the element since its 3-dB region of excitation was at the very end of the elements. This clamping in effect caused a narrowing of the 3-dB beamwidth, which gave the appearance of an increase in Q_m of 3. The discrepancies between

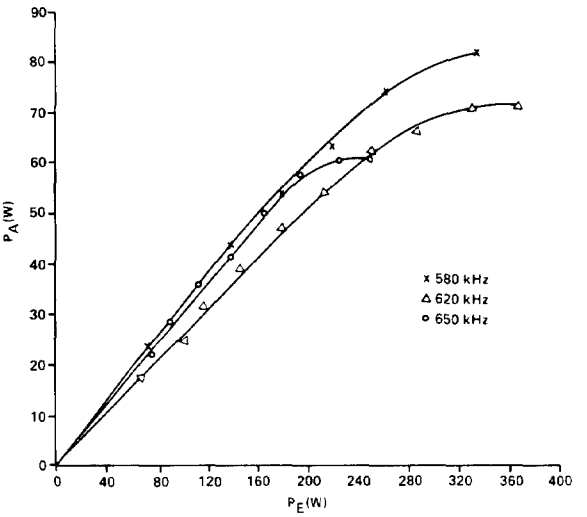

Fig. 6. Acoustical power output P_A versus electrical power input to amplifiers P_E.

the theoretical and experimental profiles at 650 kHz are attributed to this clamping effect.

The acoustical power output of the tapered phased array was measured as a function of input electrical power using the radiation force technique. The efficiency of the array was determined by measuring the acoustical power in the focused main beam, with 32 elements excited, as a function of the input electrical power supplied to the amplifiers. Fig. 6 shows the results for driving frequencies of 580, 620, and 650 kHz. The target was positioned at the focus of the array, set at (0, y, 100 mm), where the y position was determined by the driving frequency. The overall efficiency of the array and amplifiers was calculated from Fig. 6 to be approximately 28 percent. The small variations in efficiency (four percent) with frequency can be attributed to the quality of the match between the electrical impedances of the elements and the amplifiers. These plots indicate that the acoustic output at the focus started to level out at approximately 60 W at 650 kHz, 70 W at 620 kHz, and 80 W at 580 kHz. This observed increase in acoustical power output at the start of the nonlinearity with decreased frequency can be explained by examining the modes of power dissipation in the ceramic.

The power dissipation is due primarily to internal dielectric and mechanical losses which convert electrical and mechanical energy to heat. The temperature rise resulting from these losses can cause a reduction in the efficiency of the ceramic. Both dielectric and mechanical losses are proportional to frequency and, therefore, the higher the frequency (cw), the greater the power dissipation and temperature rise in the ceramic [26]. Elevated temperatures will lower the mechanical quality factor Q_m, thus reducing the efficiency of the ceramic [27].

The acoustical power output measurements were retaken with forced air cooling on the back of the elements. The cooling did not have a measurable effect on the acoustical power output of the array, which is consistent with the fact that most of the heat removal will be to the water, with or without cooling of the back surface.

VI. Conclusion

The acoustical fields predicted from the theoretical model of the tapered elements have been shown to agree well with the experimental data. With this model it is possible to design other tapered phased arrays and predict the array's acoustical output as a function of position in the y direction.

The results of the acoustical power output measurements suggest that 64 elements, with a 1.79-mm element width, and 580- to 650-kHz frequency range would produce a maximum acoustical power output ranging from approximately 120 to 160 W. For an attenuation coefficient of 0.1 Np/cm/MHz, the total acoustical power available at an 8-cm focal depth for a frequency of 650 kHz is approximately 42 W. Therefore, the maximum time-averaged intensity available to heat a 2.1-cm diameter tumor at a depth of 8 cm is approximately 12 W/cm^2. If the tumor has an absorption coefficient of 0.08 Np/cm/MHz, an absorbed power density of approximately 1.3 W/cm^3 could be produced at the 8-cm depth. Several theoretical studies suggest that absorbed power densities of 150–200 mW/cm^3 in the tumor are necessary to produce tumor temperatures of at least 43°C [14], [23]. Therefore, based on these studies, an array with 64 elements would be able to treat a 2.1-cm-diameter tumor up to 8 cm in depth with an intensity gain of 3 dB.

Since the majority of tumors one would wish to treat are greater than 2 cm in diameter, it would be desirable to modify the transducer so that it could treat larger tumors. Based on the intensity gain calculations and the acoustical power output measurements, it appears that the frequency range of the tapered phased array should be decreased in future designs. A transducer operating at a decreased frequency will be able to treat larger tumors with the same intensity gain and will have a greater acoustical power output before reaching a saturation level. The greater acoustical power output at lower frequencies is not only due to decreased internal losses, but also to the larger element widths allowable with the lower frequencies. On the other hand, a decrease in frequency will decrease the absorbed power density. For example, at 500 kHz a time-averaged intensity of 12 W/cm^2 at the tumor will produce an absorbed power density of only 960 mW/cm^3, compared to 1.3 W/cm^3 calculated for the same tumor size and location in the 650-kHz case. However, this is still well above the 200 mW/cm^3 which has been suggested as sufficient for heating tumors.

Future theoretical studies require incorporation of the bioheat equation with the predicted field intensity patterns of the tapered phased array to determine the temperature distributions expected in the irradiated tissue. With such a model the intensity gain and power deposition necessary to heat selectively a given tumor can be determined. Once this is accomplished, the required acoustical power output and frequency range of the array can be better estimated.

ACKNOWLEDGMENT

The authors wish to thank Dr. S. G. Foster, as well as S. G. Silverman, for their technical assistance, and B. McNeill for fabricating the transducer used in this study.

REFERENCES

[1] P. M. Corry, K. Jabboury, E. P. Armour, and J. S. Kong, "Human cancer treatment with ultrasound," *IEEE Trans. Sonics Ultrason.*, vol. SU-31, no. 5, pp. 444-456, 1984.

[2] C. W. Song, "Physiological factors in hyperthermia," *NCI Monograph*, vol. 61, pp. 169-176, 1982.

[3] G. M. Hahn, "Hyperthermia for the engineer: A short biological primer," *IEEE Trans. Biomed. Eng.*, vol. BME-31, no. 1, pp. 3-8, 1984.

[4] F. W. Kremkau, "Cancer therapy with ultrasound: A historical review," *J. Clin. Ultrasound*, vol. 7, pp. 287-300, 1979.

[5] G. M. Hahn, P. Kernahan, A. Martinez, D. Pounds, and S. Prionas, "Some heat transfer problems associated with heating by ultrasound microwaves, or radiofrequency," *Ann. NY Acad. Sci.*, vol. 335, pp. 327-346, 1980.

[6] D. A. Christiansen and C. H. Durney, "Hyperthermia production for cancer therapy: A review of fundamentals and methods," *J. Microwave Power*, vol. 16, pp. 89-105, 1981.

[7] P. P. Lele, "Hyperthermia by ultrasound," *Proc. Int. Symp. Cancer Therapy by Hyperthermia and Radiation*, 1975, pp. 108-178.

[8] A. K. Chan, R. A. Sigelmann, and A. W. Guy, "Calculations of therapeutic heat generated in fat-muscle-bone layers," *IEEE Trans. Biomed. Eng.*, vol. BME-21, pp. 280-294, 1974.

[9] J. B. Marmor, D. P. Pounds, T. Postic, and G. M. Hahn, "Treatment of superficial human neoplasms by local hyperthermia induced by ultrasound," *Cancer*, vol. 43, pp. 188-192, 1979.

[10] E. J. Seppi, E. G. Shapiro, and L. T. Zitelli, "Ultrasonic system for hyperthermia," Abstract AD-22, Rad. Res. Soc. Meeting, 1985.

[11] P. Fessenden *et al.*, "Experience with a multitransducer ultrasound system for localized hyperthermia of deep tissues," *IEEE Trans. Biomed. Eng.*, vol. BME-31, no. 1, pp. 126-135, 1984.

[12] P. Fessenden, *et al.*, "Analysis of deep hyperthermia treatments using six ultrasound transducers in a fixed frequency/geometry configuration," Abstract Ad-27, Rad. Res. Soc. Meeting, 1985.

[13] P. P. Lele and K. J. Parker, "Temperature distributions in tissues during local hyperthermia by stationary or steered beams of unfocused or focused ultrasound," *Brit. J. Cancer*, vol. 45, Suppl. V., pp. 108-121, 1982.

[14] R. J. Dickinson, "An ultrasound system for local hyperthermia using scanned focused transducers," *IEEE Trans. Biomed. Eng.*, vol. BME-31, pp. 120-125, 1984.

[15] K. B. Ocheltree, P. J. Benkeser, L. A. Frizzell, and C. A. Cain, "An ultrasonic phased array applicator for hyperthermia," *IEEE Trans. Sonics Ultrason.*, vol. SU-31, no. 5, pp. 526-531, 1984.

[16] P. J. Benkeser, K. B. Ocheltree, L. A. Frizzell, and C. A. Cain, "Ultrasound phased array hyperthermia applicator," *Proc. Seventh Ann. Conf. IEEE Eng. Med. Biol. Soc.*, pp. 337-340, 1985.

[17] L. A. Frizzell, P. J. Benkeser, K. B. Ocheltree, and C. A. Cain, "Ultrasound phased arrays for hyperthermia treatment," *Proc. 1985 IEEE Ultrason. Sym.*, pp. 930-935, 1985.

[18] F. L. Lizzi, *et al.*, "Therapeutic applications of a transducer with frequency controlled beam scanning," *Proc. AIUM/SDMS Ann. Convention, J. Ultrasound in Med.*, vol. 4, p. 18, 1985.

[19] A. Macovski, "Ultrasonic imaging using arrays," *Proc. IEEE*, vol. 67, no. 4, pp. 484-495, 1979.

[20] B. D. Steinberg, *Principles of Aperture and Array System Design*. New York: Wiley, pp. 305-309, 1976.

[21] T. F. Heuter and R. H. Bolt, *Sonics*. New York: Wiley, pp. 106-107, 1966.

[22] R. T. Beyer and S. V. Letcher, *Physical Ultrasonics*. New York: Academic, p. 52, 1969.

[23] R. B. Roemer, W. Swindell, S. T. Clegg, and R. L. Kress, "Simulation of focused, scanned ultrasonic heating of deep-seated tumors: The effect of blood perfusion," *IEEE Trans. Sonics Ultrason.*, vol. SU-31, no. 5, pp. 457-466, 1984.

[24] K. B. Ocheltree, "Theoretical analysis of ultrasonic linear phased arrays for hyperthermic treatment," M.S. thesis, Univ. of Illinois at Urbana-Champaign, Urbana, IL, 1984.

[25] P. J. 't Hoen, "Influence of component errors on the directivity function of pulsed ultrasonographic linear arrays," *Ultrasonics*, vol. 21, no. 6, pp. 275-279, 1983.

[26] D. A. Berlincourt, D. R. Curran, and H. Jaffe, "Piezoelectric and piezomagnetic materials and their function in transducers," *Physical Acoustics*, W. P. Mason, Ed. New York: Academic, pp. 170-267, 1964.

[27] D. A. Berlincourt, "Piezoelectric crystals and ceramics," *Ultrasound Transducer Materials*, O. E. Mattiat, Ed. New York: Plenum, pp. 63-124, 1971.

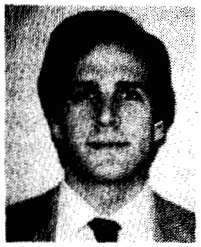

Paul J. Benkeser (S'80-M'86) was born in Lafayette, IN, on December 29, 1958. He received the B.S. degree in electrical engineering from Purdue University, West Lafayette, IN, in 1981, and the M.S. and Ph.D. degrees in electrical engineering from the University of Illinois in 1983 and 1985, respectively.

Since 1985 he has been an Assistant Professor with the School of Electrical Engineering, Georgia Institute of Technology, Atlanta. His research interests include ultrasound phased arrays, ultrasound hyperthermia, and acoustic sensors.

Dr. Benkeser is a member of Eta Kappa Nu.

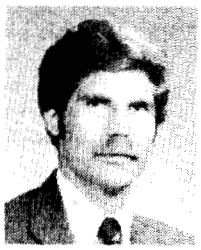

Leon A. Frizzell (S'71-M'74-SM'82) was born in West Stewartstown, NH, on September 12, 1947. He received the B.S. degree in physics from the University of New Hampshire, Durham, NH, in 1969, and the M.S. and Ph.D. degrees in electrical engineering from the University of Rochester, Rochester, NY, in 1971, and 1976, respectively.

Since 1975 he has been in the department of electrical and computer engineering at the University of Illinois at Urbana-Champaign, where he is currently an Associate Professor of electrical engineering and of bioengineering. His research interests include ultrasonic tissue characterization, ultrasonic biological effects, hyperthermia, and ultrasonic bioengineering.

Dr. Frizzell is a member of the Acoustical Society of America, the American Association for the Advancement of Science, the North American Hyperthermia Group, Sigma Xi, and is a Fellow of the American Institute of Ultrasound in Medicine.

Kenneth B. Ocheltree (S'82-M'82-S'82-M'86) was born on June 8, 1960, in Norfolk, VA. He received the B.S. degree in electrical engineering from Virginia Polytechnic Institute in 1982 and the M.S. degree in electrical engineering from the University of Illinois at Urbana-Champaign in 1984. He is currently attending the University of Illinois while studying for the Ph.D. degree in electrical engineering. His research interests are related to hyperthermia, in particular the application of phased arrays and bioheat transfer analysis.

Charles A. Cain (S'65-S'71-M'71-SM'80) was born in Tampa, FL, on March 3, 1943. He received the B.E.E. (highest honors) degree from the University of Florida, Gainesville, in 1965, the M.S.E.E. degree from the Massachusetts Institute of Technology, Cambridge, in 1966, and the Ph.D. degree in electrical engineering from the University of Michigan, Ann Arbor, in 1972.

During 1965-1968, he was a member of the Technical Staff at Bell Laboratories, Naperville, IL, where he worked in the electronic switching systems development area. Since 1972, he has been in the Department of Electrical and Computer Engineering, University of Illinois at Urbana-Champaign, where he is currently Professor of Electrical Engineering and Bioengineering and Chairman of the Bioengineering Faculty. He has been involved in Research on the biological effects and medical applications of microwaves and ultrasound.

Dr. Cain is currently an Associate Editor of *Radiation Research*.